Particuology xxx (2018) xxx–xxx

Contents lists available at ScienceDirect

Particuology

journal homepage: www.elsevier.com/locate/partic

Particle penetration in fiber filters

Norbert Riefler[a,*], Martina Ulrich[b], Marko Morshäuser[b], Udo Fritsching[a,c]

[a] Process Engineering, Institute of Materials Science, Badgasteiner Strasse 3, 28359 Bremen, Germany
[b] Lydall Gutsche GmbH & Co. KG, Hermann-Muth-Str. 8, 36039 Fulda, Germany
[c] Particles and Process Engineering, University of Bremen, Bibliothekstrasse 1, 28359 Bremen, Germany

ARTICLE INFO

Article history:
Received 30 June 2017
Received in revised form 8 November 2017
Accepted 16 November 2017
Available online xxx

Keywords:
Particle filtration
Fiber filter
X-ray microtomography
Computational fluid dynamics–discrete element method coupling
High-fidelity simulation
Transient mesh morphing

ABSTRACT

Particle separation from gases is an important unit operation in manifold industrial applications, such as those conducted in environmental protection. For analysis of particle penetration and separation in fiber filters, standard dust particles (Al_2O_3) were loaded in the gas flow of a filter test facility and deposited within new and uncharged fiber filters. The loaded filters were analyzed by micro-computer tomography and scanning electron microscopy. Three-dimensional tomograms of the samples show an exponential decay of the penetration depth of the particles. This dependency is confirmed by simulations conducted using the discrete element method coupled with computational fluid dynamics within unloaded and loaded fiber structures. Microscale processes of particle separation at the fibers as well as the filtration efficiency and time-dependent filtering process are derived from the simulations. Local particle clustering in the filter medium and partial filter clogging are thus identified.

Introduction

Processes in both industry and daily life produce exhausts that contain particles that need to be removed before reaching the atmosphere. Within the cement industry, aramid fiber filters can filter particles from hot gas streams using porous aramid fiber filter media because of the specific heat resistances of the media. Different filters, such as woven textiles, porous foams, nucleopore membranes, and nonwoven fiber filters, may be used. Relevant in situ parameters, including the penetration depth of particles, the preferential separation of particles at certain locations in the filter, and the spatial structure of the filter medium, and dynamic effects, such as the change in the fiber capture coefficient during deposition and/or filter clogging, are difficult to obtain experimentally. Bourrous et al. (2014) investigated the penetration depth of nanoparticles within EPA (efficient particulate air), and HEPA (high efficiency particulate air) filters. They found an exponential penetration profile in the scanning electron microscopy (SEM) of filter cross sections. A three-dimensional (3D) X-ray tomography method with 1-μm pixel resolution was applied by Jackiewicz, Jakubiak, and Gradoń (2015) to self-made polypropylene fiber filters. They observed a decrease in particle deposition for different clean gas flow velocities in the direction of the particle-laden flow. Another 3D tomography method based on nuclear magnetic resonance yielded images of the fiber structure with a voxel resolution of 59 μm (Hoferer, Lehmann, Hardy, Meyer, & Kasper, 2006). Gervais, Bemer, Bourrous, and Ricciardi (2017) obtained 3D synchrotron X-ray tomograms for fiber filters used as descriptorsto generate fiber structures that were used to verify simula-tions with a voxel-based fluid dynamic solver (GeoDict). Hellmann, Schmidt, Ripperger, Thelen, and Möhlmann (2012) compared simulations performed with the software package DNSlab and their experimental findings based on measurements of particle numbers made before and after the investigated filter media. Herman, Lehmann, and Velu (2006) calculated pressure drops of two-dimensional fiber packings using a standard computational fluid dynamics (CFD) tool (Fluent) and compared the results with those obtained using Kuwabara and cellular models. Collection efficiencies and pressure drops were calculated with the same solver by Hosseini and Tafreshi (2010), who compared two-dimensional simulations with 3D simulations.

The present paper investigates the loading process of nonwoven aramid fiber filters using a coupled CFD–discrete element method (DEM) procedure including mesh-morphing and compares the results with experimental results of the same process obtained through microtomography (μ-CT). After a description of the preparation, the experimentally determined depositions and penetration depths of particles are presented for different charging times. The

* Corresponding author.
E-mail address: riefler@iwt.uni-bremen.de (N. Riefler).

https://doi.org/10.1016/j.partic.2017.11.008
1674-2001/

Nomenclature

A	Collection area (m^2)
c_p	Particle concentration (g/m^3)
d_f	Fiber diameter (m)
d_p	Particle diameter (m)
D	Diffusion coefficient (m^2/s)
F_D	Drag force (N)
f_l	Length of fiber (m)
k_B	Boltzmann constant (J/K)
$L_{x,y}$	Dimensions of packing (m)
L_z	Packing length (along direction of flow) (m)
m_l	Mass load of charged particles (g/m^2)
$m_{p,all}$	Mass of all charged particles (g/m^2)
N_d	Number of deposited particles
N_p	Number of particles having passed through the filter
r_d	Randomness of the fiber segment direction
Re	Reynolds number
s_l	Length of fiber segments (m)
T	Tortuosity; temperature (K)
t_{dep}	Deposition time (s)
u_0	Approach velocity (m/s)
x,y,z	Coordinates (m)
Greeks	
α	Solid fraction
ε	Porosity
η	Fractional collection efficiency (%)
κ	Permeability (m^2)
μ	Dynamic viscosity (Pa s)
ρ	Density (kg/m^3)
θ_f	Fiber direction (°)
$\zeta/em>$	Stokes drag coefficient
ζ_D	Drag coefficient

deposition curves are analyzed from two separate X-ray μ-CT results, as just two measurement series for different measurement devices are performed. The model-based generation of fiber packings for the meshing with straight and curved fibers is then described. The pressure drops of these (unladen) fiber structures and specifically generated sphere packings are used to verify the meshing process and quality by making comparisons with Davies (Thomas, Penicot, Contal, Leclerc, & Vendel, 2001) and Ergun (1952) correlations, respectively. After a description of the particle deposition method, results obtained from μ-CT and simulations are compared.

Experimental characterization

Sample preparation

Samples of fiber packings of aramid fibers were investigated. This filter medium consisted of fibers having a mean diameter of $d_f = 15\,\mu m$, which were applied to the lower and upper sides of a supporting fabric by a needle punching machine. Fig. 1 is an image of the cross section of an unloaded fiber filter while Fig. 2 is a sketch of the filter structure. Pural NF Al_2O_3 particles with $d_{50,3} = 4\,\mu m$ were used as charging dust in filtration experiments; see the particle size distribution in Fig. 3.

Three particle-laden samples were prepared using a test filtration stand according to VDI guideline 3926 'Testing of cleanable filter media—standard test for the evaluation of cleanable filter media' published by Lydall Gutsche GmbH & Co. KG, Fulda (Germany). The particle concentration of the gas flow was

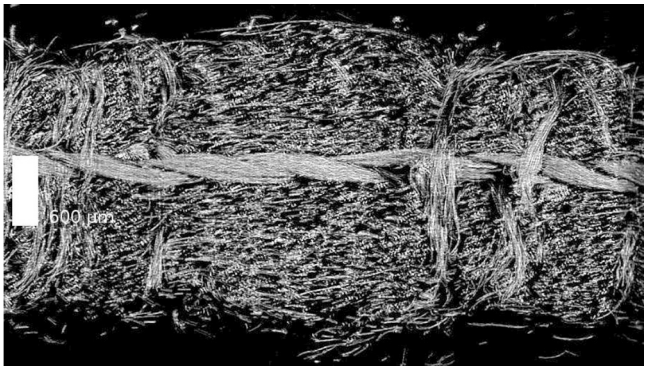

Fig. 1. Cross section of X-ray μ-CT of an uncharged fiber filter.

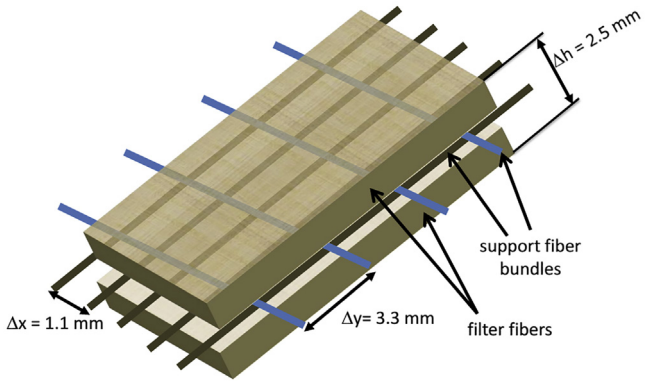

Fig. 2. Structure and composition of the investigated fiber filters.

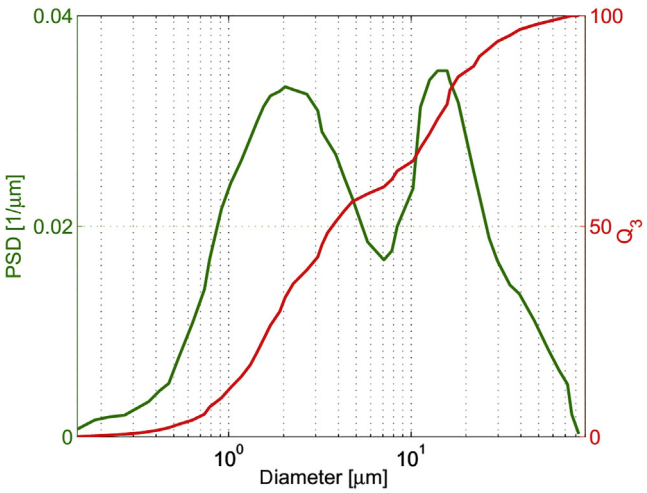

Fig. 3. Particle size distribution (PSD) and cumulative size distribution (Q_3) of Pural NF Al_2O_3 particles.

$c_p = 4.5\,g/m^3$. The first and second samples were always new, uncharged fiber packings with deposition times of 100 and 200 s, respectively. The third sample was a fully aged fiber packing that has been loaded in thousands of deposition and pulse-jet cleaning cycles (as directed by the guidelines). None of the samples were exposed to the cleaning pressure surge at the end of the cycle, and the samples were charged only until the cake formation started. In addition, μ-CT of an uncharged filter sample (see the cross section in Fig. 1 as an example) was conducted for reference.

To avoid the loss of deposited particles (e.g., during transportation), the deposited particles have to be fixed during sample preparation for analysis using a suitable method (Chi, Ji, Sun, & Cui,

Please cite this article in press as: Riefler, N., et al. Particle penetration in fiber filters. *Particuology* (2018), https://doi.org/10.1016/j.partic.2017.11.008